ACS APPLIED MATERIALS & INTERFACES

Research Article

www.acsami.org

A Novel TiO_2 Tape for Fabricating Dye-Sensitized Solar Cells on Universal Conductive Substrates

Jie Shen, Rui Cheng, Yiwei Chen, Xiaohong Chen, Zhuo Sun, and Sumei Huang*

Engineering Research Center for Nanophotonics & Advanced Instrument, Ministry of Education, Department of Physics, East China Normal University, North Zhongshan Rd. 3663, Shanghai 200062, P. R. China

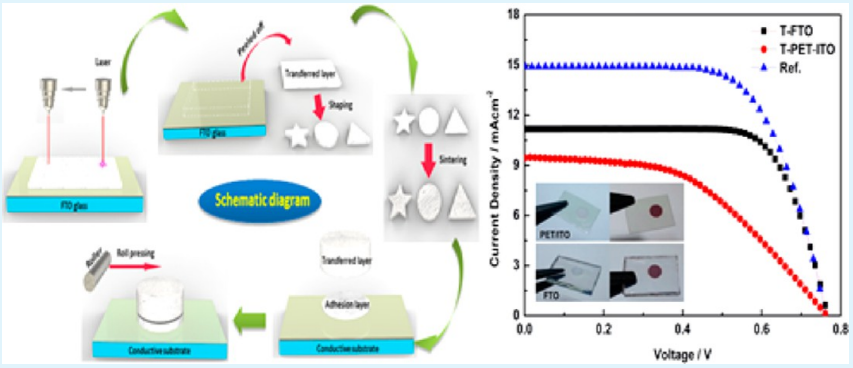

ABSTRACT: The present paper describes a new method for manufacturing large scale, stable, transportable, and designable nanostructured porous TiO_2 tapes on various substrates for use in photoelectrochemical cells. The method involves predeposition of TiO_2 strips on the fluorine doped tin oxide (FTO) glass by screen-printing method, peeling off TiO_2 strips from the substrate by a novel laser-assisted lift-off technique, sintering the formed TiO_2 tapes at 500 °C for 15 min, and compressing the sintered TiO_2 tapes on different conductive substrates with a low pressure rolling press to form mechanically stable, electrically conducting, porous nanostructured TiO_2 electrodes at room temperature. Photoelectrochemical characteristics of the resulted electrodes are presented. Dye-sensitized solar cells (DSSCs) with the as-fabricated TiO_2 photoanodes on PET-ITO and FTO glass achieved a conversion efficiency of 4.2% and 6.2%, respectively. The potential use of this new manufacturing method in future DSSC applications is discussed.

KEYWORDS: *laser-assisted lift-off, TiO_2 tape, low temperature, rolling press, layer transfer, dye-sensitized solar cell*

INTRODUCTION

After decades of research and development, dye-sensitized solar cells (DSSCs) have been proved to be a promising alternative for the development of next generation solar cells due to their respectable power conversion efficiency and potential low-cost.[1−3] Compared with other kinds of solar cells, the assembled DSSCs can be translucent and multicolored by choosing different dyes or adjusting the TiO_2 pastes, electrolytes, and counter electrodes.[4] These features make the DSSCs have a more beautiful appearance. Moreover, manufacturing the cells on low-cost plastic substrates would not only inherit the translucent and multicolored features but also enable significant cost reduction as well as roll-to-roll mass production. Flexible DSSC substrates are especially attractive for Building Integrated Photovoltaics (BIPV). Therefore, research efforts on the design and fabrication of flexible DSSCs have been emphasized.[5−7]

The porous TiO_2 photoanode is one of the most critical components in the DSSC. DSSCs based on nanoporous TiO_2 electrode on rigid glass substrate have shown the conversion efficiency of over 12%.[2] However, the fabrication steps for photoanodes in these highly efficient cells generally require a 450−500 °C sintering process,[8] which is not suitable for the widely used plastic substrates like ITO/PET and ITO/PEN as the substrate can only sustain temperature up to 150 °C.[9] Thus, much effort has been made to develop the crystalline titania network structure and fabricate plastic DSSCs at low temperature.[8,10−23] Among these technologies, mechanical compressing and transferring were the two most effective methods for fabricating plastic-based DSSCs. Yamaguchi et al. obtained a validated high efficiency of 7.4% using a mechanical compression method in 2007.[24] In this work, they made a special pretreatment of the plastic surface and prepared a modified binder free paste for the cell. Later in 2010, they used a uniaxial compressing technology to increase the efficiency to 8.1%.[25] In order to realize the strong chemical bonding between TiO_2 nanoparticles and further improve the charge transporting, a "lift-off" technology was reported by Dürr and co-workers.[16] A sintered TiO_2 layer was separated by dissolving an exhausting layer of Au between TiO_2 layer and glass, and then the separated TiO_2 layer was transferred on a plastic

Received: September 4, 2013
Accepted: December 2, 2013
Published: December 2, 2013

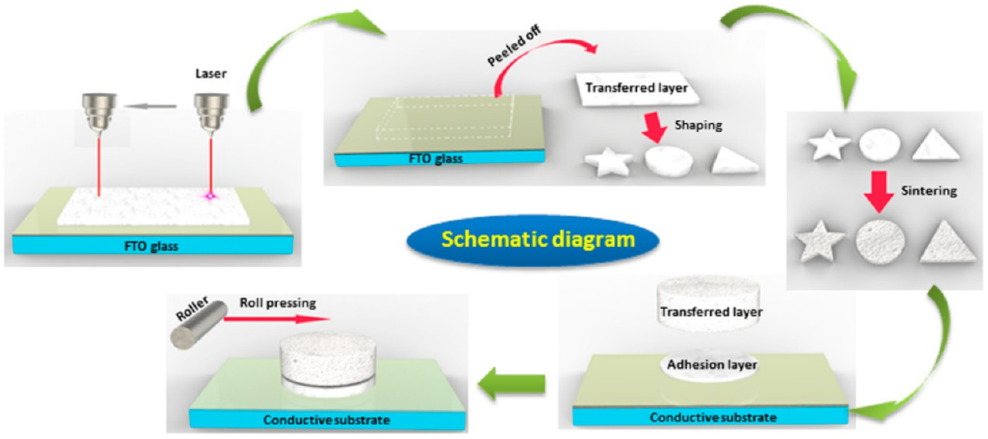

Figure 1. Schematic diagram of procedures of the laser-assisted layer transfer process.

substrate by compressing. The assembled cell achieved an efficiency of 5.8%. Another transfer method for fabricating a cosensitized multilayered photoanode was reported by Miao.[26] Using this friction-based transfer technique, two TiO_2 layers which loaded two complementary dyes were compressed together to form the multilayered photoanode. The DSSC with this composite photoanode realized much broader light harvesting of the solar spectrum and good contact with the substrate achieved a high efficiency of 11.05%. In the conventional compressing method, a high static pressure (50−150 MPa) was usually employed for good and high quality necking TiO_2 photoanode.[8,27,28] But this pressing process with high pressure has a high request for the fabrication equipment and easily leads to the irreversible destruction of the flexible conductive substrates and, thus, faces significant scaling challenges.

In this paper, a novel laser-assisted layer transfer technique for fabricating DSSCs on different substrates was reported. A designable, portable, scalable, and flexible TiO_2 tape was first prepared by a laser-assisted lift-off (LLO) method. The as-fabricated TiO_2 tape was easily cut into any designed shape. After a high temperature treatment, the sintered TiO_2 tape was firmly attached on a target conductive substrate via a low pressure rolling press process. DSSCs prepared by the as-fabricated TiO_2 photoanodes on FTO and PET-ITO substrates showed a conversion efficiency of 6.2% and 4.2%, respectively. The performance of the former is comparable to that (7.4%) of the cell prepared by the conventional high temperature method.

EXPERIMENTAL SECTION

The procedures of the laser-assisted layer transfer process are illustrated in Figure 1. Double-layered TiO_2 with a total thickness of about 14 μm was first deposited on the fluorine doped tin oxide (FTO) glass by screen-printing method using pastes containing organic binders. The pastes were prepared according to the procedures described in our previous work.[29] Then, a commercialized laser engraving machine (HT-DP50) was used to process flexible TiO_2 tapes.

The laser source is a Nd:YAG pulsed laser. The laser beam was incident normally on the surface of the screen-printed TiO_2 film using laser parameters (λ = 1064 nm, repeating frequency = 20 kHz, output power = 20 W, scanning speed = 150 mm/s, and spot size = 50 μm). The TiO_2 ribbon was detached from the FTO substrate by exposing it to the laser scanning beam at one time. The obtained TiO_2 ribbon was freestanding, tough and flexible enough to be transported and cut into any designed shape TiO_2 sheets. Next, a sintering process was performed by heating the as-fabricated TiO_2 tapes at 500 °C for 15 min. This high temperature process was carried out to further promote framework crossing-linkage to form highly crystallized mesoporous TiO_2 films having desired properties such as high porosity with good necking of the crystallite. After that, prior to transfer the sintered TiO_2 tape to a target conductive substrate, a paste containing 0.2 g P25, 5 mL ethanol and 50 μL titanium butoxide was used to deposit a thin adhesion layer on the top surface of the target substrate in order to enhance the bonding strength between the TiO_2 tape and the conductive substrate. Last, the as-transferred TiO_2 layer was mechanically pressed by rolling a rod (diameter 4 cm, length 20 cm) across the surface of the TiO_2 film for one time at room temperature. The applied vertical pressure on the top surface of the TiO_2 was about 50 kg, and the rolling speed was about 1 cm/s. Finally, the transferred TiO_2 electrodes were immersed into the dye solution (0.5 mM N719 (Solaronix) in acetonitrile and *tert*-butyl alcohol (volume ratio of 1:1)) at room temperature for 20 h. After being rinsed with acetonitrile, the TiO_2 anodes were assembled with the Pt counter-electrodes prepared by the hydrolysis process.[21] Two types of DSSCs were prepared by using the transferred TiO_2 photoelectrodes on FTO and PET-ITO glass substrates. Besides, DSSC on FTO prepared by the conventional high temperature method was fabricated as the reference cell. The three types of TiO_2 photoanodes were denoted as T-FTO, T-PET-ITO, and ref, respectively.

The structure of the TiO_2 layer before and after the laser peeling process was identified via X-ray diffractometer (XRD, Bruker D8 Davinci instrument, Cu Kα: λ = 0.15406 nm). The morphologies of transferred TiO_2 and bottom adhesion layers were characterized by using a field emission scanning electron microscope (FESEM, Hitachi S4800). The thickness of the layers were measured by using a profilometer (Dektak 6M). Electrochemical impedance spectroscopy (EIS) measurements of DSSCs were recorded with a galvanostat (PG30.FRA2, Autolab, Eco Chemie B. V Utrecht, Netherlands) under illumination 100mW cm^2. The frequency range was from 0.1 to 100 kHz. The applied bias and ac amplitude were set at open-circuit voltage (V_{oc}) of the DSCs and 10 mV between the Pt CE and the TiO_2 working electrode, respectively. Photocurrent−voltage (I−V) measurements were performed using an AM 1.5 solar simulator equipped with a 1000 W xenon lamp (model no. 91192, Oriel). The solar simulator was calibrated by using a standard silicon cell (Newport). The light intensity was 100 mW cm^2 on the surface of the test cell. I−V curves were measured using a computer-controlled digital source meter (Keithley 2440).

RESULTS AND DISCUSSION

The proposed process is a significantly flexible and fast method. It is the laser-induced delamination of TiO_2 layers from the transparent FTO substrate, or laser lift-off (LLO) for short. The proposed method is fundamentally based on the laser-

induced thermal desorption and is different from the traditional LLO technology.[30−32] For example, the widely reported LLO technology for the production of freestanding GaN epitaxial layers was based on the laser induced-thermal decomposition of the irradiated GaN interfacial layer into metallic Ga and gaseous N_2.[33] In our work, the nanostructured film adhered to the substrate can be desorbed when the thermoelastic force, caused by a rapid thermal expansion of the film resulting from pulsed laser irradiation, exceeds the adhesive force (predominantly van der Waals force) between the film and the substrate. In this process, the incident laser beam is mostly absorbed by the organic binders in the predeposited TiO_2 film, and slightly by the FTO layer.

Figure 2a shows an image of the laser processed sample. The process was carried out by scanning the laser beam on one

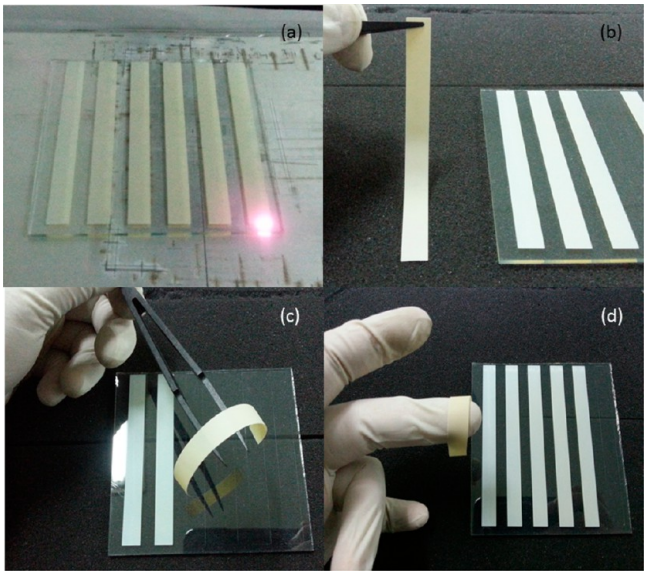

Figure 2. (a) Photo of the sample during laser scanning processing; (b−d) photos of the peeled off "TiO_2 tape" with high flexibility.

screen-printed TiO_2 strip at one time. The laser beam spot is clearly displayed in the figure. The predeposited TiO_2 strips can be easily peeled off from the FTO glass substrate without any damage after the laser scanning processing. Figures 2b−d shows the images of obtained TiO_2 tapes. They are freestanding, touchable, and bendable. The formed TiO_2 tapes can be stored and transported. Meanwhile, the bendable TiO_2 tape shows such a high ductility that it can be easily cut into any designed shape. In combination with post heat treatment and low pressure roll-presssing techniques, the LLO technology for production of TiO_2 tapes provide us with a new and facile method for fabricating large-area and high performance flexible DSSCs in mass production.

The XRD patterns of TiO_2 layers before and after peeling off the FTO glass by laser-assisted lift-off technology are shown in Figure 3. P25 (P25, Degussa) powders were used as a reference. The XRD result of P25 powders shows intense TiO_2 anatase and relatively weak rutile phases. The anatase phase signals shown in P25 were clearly observed in the TiO_2 layers before and after laser treatment, while the weak TiO_2 rutile phase signals in P25 were not very obviously detected in these TiO_2 layers due to the existence of organic materials in the latter. Additionally, compared with the case of the TiO_2 layer without laser treatment, the peeled TiO_2 after laser

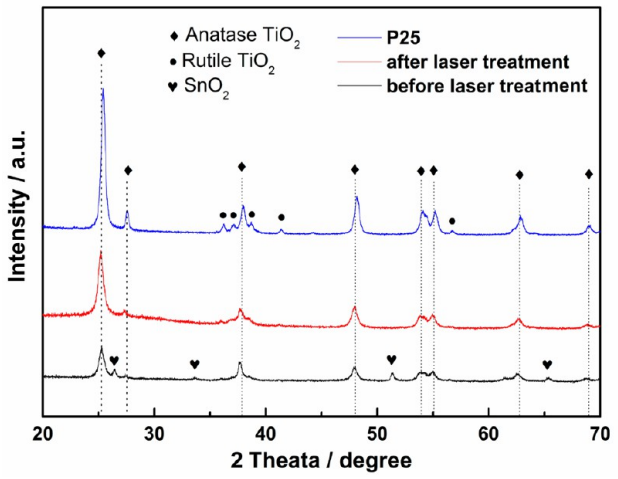

Figure 3. XRD patterns of TiO_2 layers before and after laser scanning processing.

treatment shows stronger anatase peaks. This result could be attributed to the laser induced-thermal decomposition of some organic binders in the predeposited TiO_2.

Figure 4 displays the cross-sectional SEM images of the transferred TiO_2 electrode on FTO glass. From Figure 4a, the transferred TiO_2 and bottom adhesion layers can be clearly distinguished and no obvious cracks were found in both films. The result indicates that the transferred TiO_2 layer is firmly adhered to the FTO substrate by the low pressure roll-pressing treatment. More details about the transferred TiO_2 are shown in the SEM images (b−d) with a higher magnification. Compared with the bottom adhesion layer, the transferred TiO_2 layer in Figure 4d has an obvious network structure. It demonstrates the low pressure pressing treatment did not destroy the network structure which was formed by the previous high temperature sintering. The inherited porous network structure ensures a good electron transport property of the transferred TiO_2 photoanode. On the top of the transferred TiO_2 layer, a scattering layer composed of large TiO_2 particles is found in Figure 4c. This layer was applied to improve the conversion efficiency by increasing the path length of the incident light in the photoanode.[34]

Generally, the porosity of the porous TiO_2 layer will be decreased after a high pressure pressing treatment. To study the influence of our low pressure roll-pressing treatment on the transferred TiO_2 photoanode, the amount of dye adsorbed on the photoelectrode was measured by desorption in 0.1 M NaOH aqueous solution. Figure 5 illustrates the absorbance spectra of the solutions containing dyes detached from T-FTO, T-PET-ITO, and ref photoanodes. From figure 5, the three types of photoanodes exhibit nearly identical absorbance. The TiO_2 electrode prepared by the conventional sintered method only shows a little higher absorption intensity at 512 nm. As is well-known, the amount of dye loading on the TiO_2 film is mainly related to the surface area of the TiO_2 nanostructures. Dye adsorption measurement results in Figure 5 indicate our low pressure roll-pressing treatment only has a slightly negative influence on the porosity of the porous TiO_2 layer. Therefore, as a film transfer technique, our low pressure roll-pressing process has an advantage in fabrication DSSCs with a high current density.

Figure 6 shows photocurrent density−voltage (J−V) curves of DSSCs fabricated with the transferred and the conventional

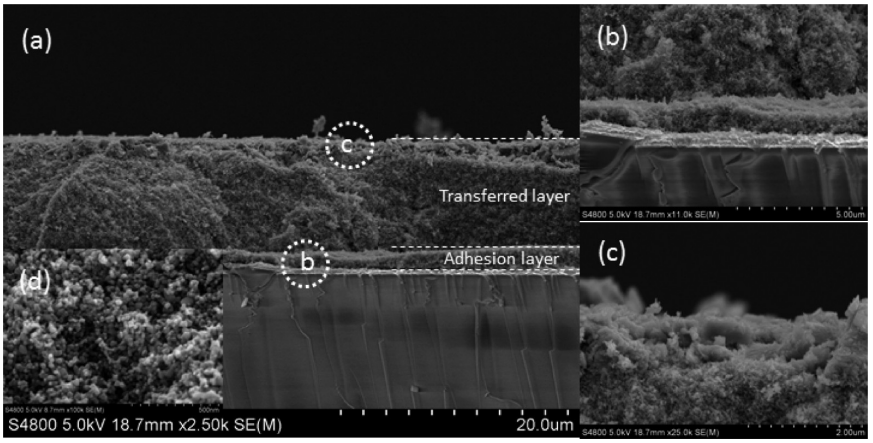

Figure 4. (a) Cross-sectional SEM image of the TiO_2 layer transferred on the FTO substrate and (b–d) magnified SEM images of the interface.

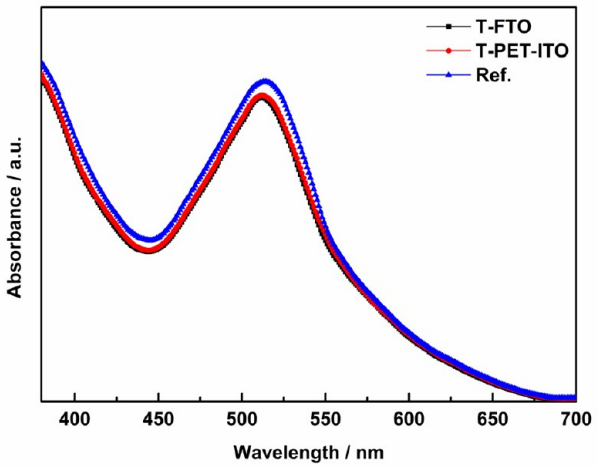

Figure 5. Optical absorbance of solutions containing dyes detached from three types of TiO_2 photoanodes.

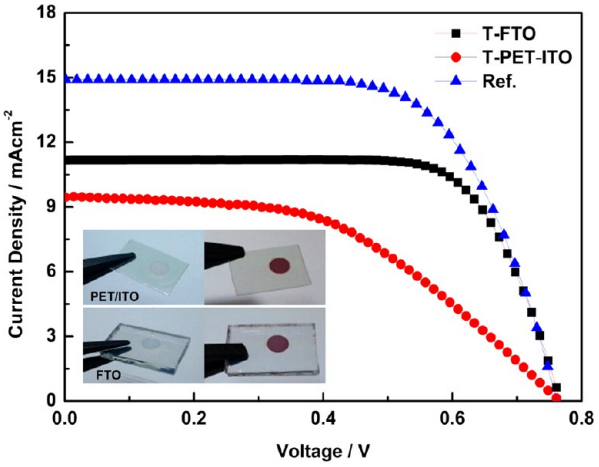

Figure 6. J–V curves of DSSCs fabricated with three types of TiO_2 photoanodes (inset: photos of T-FTO and T-FET-ITO samples before and after dye loading).

sintered TiO_2 photoanodes. The detailed characteristcs of these cells are summarized in Table 1.

As shown in Figure 6 and Table 1, the DSSC based on T-FTO exhibits a short-circuit photocurrent density (J_{sc}) of 11.2 mA cm^{-2}, a fill factor (FF) of 72.5%, an open-circuit voltage (V_{oc}) of 0.767 V, and a conversion efficiency of 6.2%. This performance is higher than that of the device based on T-PET-ITO (4.2%), and quite comparable to that (7.4%) of the reference cell using the conventional sinterred TiO_2 photoanode.

Table 1. J–V Characteristics of the DSSCs with the Transferred and the Conventional Sintered TiO_2 photoanodes

photoanode	J_{sc} (mA cm^{-2})	V_{oc} (V)	FF (%)	η (%)
T-FTO	11.2	0.767	72.5	6.2
T-PET-ITO	9.9	0.766	56.7	4.2
ref	14.9	0.764	69.7	7.4

To understand the difference in J–V performance of DSSCs fabricated with three types of photoanodes, EIS measurements were carried out under constant light illumination (100 mW cm^{-2}) biased at open-circuit conditions. Figure 7 shows the impedance spectra of the DSSCs with three kinds of photoanodes. Figure 7a shows the Nyquist plots of these devices. The obtained spectra were fitted with Nova software (v1.9, Metrohm Autolab) in terms of the equivalent circuit shown in the inset of Figure 7a. The ohmic serial resistance (R_s) corresponds to the overall series resistance. The first and second semicircles correspond to the charge-transfer resistance levels at the counter electrode (R_{ct1}) and at the TiO_2/dye/electrolyte interface (R_{ct2}), respectively. The third circle represents the Warburg diffusion process in the electrolyte (R_{ct3}).[35,36] Compared with the series resistance (R_s) values of DSSCs with ref (12.6 Ω) and T-FTO (12.4 Ω), the DSSC based on T-PET-ITO photoanode shows a much higher R_s (16.5 Ω). The higher R_s could be caused by the deformation of the substrate during the roll-pressing process. Although the DSSC with T-FTO shows a little lower R_s than that of the cell based on the conventional sintered photoanode, the former displays a higher R_{ct2} (9.4Ω) than that (6.7Ω) of the latter. Both R_s and R_{ct2} made contribution to the internal series resistance, and their total effect resulted in the lower fill factor and the smaller energy conversion efficiency in the former device, shown in Figure 6a and Table 1.

Figure 7b shows the corresponding Bode plots of the DSSCs fabricated with three types of photoanodes. Generally the Bode phase plots of DSSC contain three characteristic frequency peaks from low frequency to high frequency. Among these peaks, the middle-frequency (1–100 Hz) band is correspond-

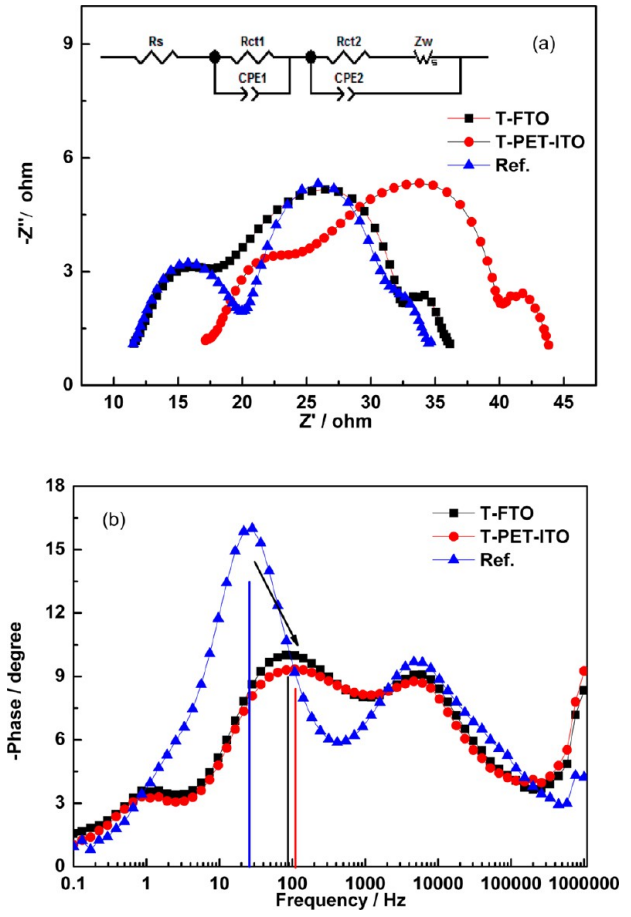

Figure 7. Impedance spectra of DSSCs with three types of photoanodes. (a) Nyquist plots and (b) Bode phase plots.

ing to the TiO_2/dye/electrolyte interface. The peak frequency in this middle band is related to the charge recombination rate, and its reciprocal is regarded as electron lifetime. From the Bode plots of Figure 7b, the conventional cell shows a lower peak frequency than that of the T-FTO or T-PET-ITO based cell in the middle-frequency region, indicating that the electron lifetime in the device based on either of the transferred TiO_2 photoanodes is shorter than the conventional sintered based DSSC. The preparation of the TiO_2 tape based photoanode involved using a paste containing organic binders to form the adhesion layer between the TiO_2 layer and the target substrate. Impurities or defects would act as the recombination centers. The shorter lifetime of the T-PET-ITO anode could be caused by impurities or defects in the adhesion layer and the bad contact on the substrate, leading to enhanced recombination among the interfaces.

Our work has demonstrated that the reported method for the fabrication of novel TiO_2 tapes has an enormous potential for the development of the flexible DSSC technology. One important advantage with the method is the capability of continuous manufacturing of the nanostructured porous film. Additionally, the proposed low pressure rolling press makes it more prominent. Another major advantage is that all the main and key steps of the method are very fast and controllable, thereby allowing very high output, especially when adopted in a mass production process. Nevertheless, the preparation of the TiO_2 tape based photoanode involves using a paste containing organic binders to form the adhesion layer between the TiO_2 layer and the target substrate. Impurities or defects would act as the recombination centers, which might increase the dark current so as to decrease the fill factor of the device. Moreover, the interelectrode contact resistance arising from poor interfacial adhesion is responsible for a considerable portion of the total resistance in the flexible DSSC. Thus, it is very important to eliminate as many sources of potential contamination as possible during the photoanode fabrication processes, and to make sure to completely bridge the gap between the TiO_2 layer and the target substrate and improve short-circuit photocurrent by reducing the contact resistance. Enhancing fill factor and short-circuit photocurrent can significantly increase the efficiency of TiO_2 tape based DSSCs. Therefore, the photoelectric efficiencies of TiO_2 tape based DSSCs can be improved by enhancing the adhesion between the TiO_2 layer and the substrate. Further studies on the synthesis of high viscosity TiO_2 paste without using organic binders for adhesion layer coating or the design of additional treatments to remove the residual organics in the adhesion layer need to be carried out to make the proposed novel transfer method more practical and effective.

CONCLUSIONS

In summary, we have reported a novel laser-assisted layer transfer method for fabricating a stable and flexible TiO_2 tape. The as-fabricated TiO_2 tape is ductile and tough enough to be conveniently stored and transported. It can be cut into any designed shape TiO_2 sheets. A high temperature treatment was employed to change the TiO_2 tapes into highly crystallized mesoporous TiO_2 ones having desired properties such as high porosity with good necking of the crystallite. Combining with a low pressure roll press, the sintered TiO_2 layer is transferred onto the target substrate. Two types of transferred TiO_2 photoanodes on the FTO and PET-ITO substrates were prepared. The cells fabricated with these two kinds of photoanodes achieved an overall energy conversion efficiency of 6.2% and 4.2% in full sunlight.

AUTHOR INFORMATION

Corresponding Author

*E-mail: smhuang@phy.ecnu.edu.cn. Tel: 86 21 62233227. Fax: 86 21 62232053.

Notes

The authors declare no competing financial interest.

ACKNOWLEDGMENTS

This work was supported by National Natural Science Foundation of China (No. 11274119, 61275038).

REFERENCES

(1) Grätzel, M. *Nature* **2001**, *414*, 338−344.
(2) Yella, A.; Lee, H.-W.; Tsao, H. N.; Yi, C.; Chandiran, A. K.; Nazeeruddin, M. K.; Diau, E. W.-G.; Yeh, C.-Y.; Zakeeruddin, S. M.; Grätzel, M. *Science* **2011**, *334*, 629−634.
(3) Fredin, K.; Nissfolk, J.; Hagfeldt, A. *Sol. Energy Mater. Sol. Cells* **2005**, *86*, 283−297.
(4) Weerasinghe, H. C.; Huang, F.; Cheng, Y.-B. *Nano Energy* **2012**, *2*, 174−189.
(5) Grätzel, M. *Prog. Photovoltaics Res. Appl.* **2006**, *14*, 429−442.
(6) Yoon, S.; Tak, S.; Kim, J.; Jun, Y.; Kang, K.; Park. *J. Build. Environ.* **2011**, *46*, 1899−1904.
(7) Grätzel, M. *Philos. Trans. R. Soc., A.* **2007**, *365*, 993−1005.

(8) Lindström, H.; Holmberg, A.; Magnusson, E.; Lindquist, S.-E.; Malmqvist, L.; Hagfeldt, A. *Nano Lett.* **2001**, *1*, 97−100.
(9) Zardetto, V.; Brown, T. M.; Reale, A.; Di Carlo, A. *J. Polym. Sci., Part B: Polym. Phys.* **2011**, *49*, 638−648.
(10) Zhang, D.; Downing, J. A.; Knorr, F. J.; McHale, J. L. *J. Phys. Chem. B* **2006**, *110*, 21890−21898.
(11) Li, K.; Luo, Y.; Yu, Z.; Deng, M.; Li, D.; Meng, Q. *Electrochem. Commun.* **2009**, *11*, 1346−1349.
(12) Miyasaka, T.; Ikegami, M.; Kijitori, Y. *J. Electrochem. Soc.* **2007**, *154*, A455−A461.
(13) Ferrere, S.; Gregg, B. A. *J. Phys. Chem. B* **2001**, *105*, 7602−7605.
(14) Park, N. G.; Kim, K. M.; Kang, M. G.; Ryu, K.; Chang, S.; Shin, Y. J. *Adv. Mater.* **2005**, *17*, 2349−2353.
(15) Grinis, L.; Dor, S.; Ofir, A.; Zaban, A. *J. Photochem. Photobiol., A* **2008**, *198*, 52−59.
(16) Dürr, M.; Schmid, A.; Obermaier, M.; Rosselli, S.; Yasuda, A.; Nelles, G. *Nat. Mater.* **2005**, *4*, 607−611.
(17) Rawolle, M.; Niedermeier, M. A.; Kaune, G.; Perlich, J.; Lellig, P.; Memesa, M.; Cheng, Y.-J.; Gutmann, J. S.; Müller-Buschbaum, P. *Chem. Soc. Rev.* **2012**, *41*, 5131−5142.
(18) Orilall, M. C.; Wiesner, U. *Chem. Soc. Rev.* **2011**, *40*, 520−535.
(19) Snaith, H. J.; Schmidt-Mende, L. *Adv. Mater.* **2007**, *19*, 3187−3200.
(20) Rawolle, M.; Braden, E. V.; Niedermeier, M. A.; Magerl, D.; Sarkar, K.; Fröschl, T.; Hüsing, N.; Perlich, J.; Müller-Buschbaum, P. *ChemPhysChem* **2012**, *13*, 2412−2417.
(21) Nilsson, E.; Sakamoto, Y.; Palmqvist, A. E. *Chem. Mater.* **2011**, *23*, 2781−2785.
(22) Haseloh, S.; Choi, S. Y.; Mamak, M.; Coombs, N.; Petrov, S.; Chopra, N.; Ozin, G. A. *Chem. Commun.* **2004**, No. Issue 13, 1460−1461.
(23) Shibata, H.; Ogura, T.; Mukai, T.; Ohkubo, T.; Sakai, H.; Abe, M. *J. Am. Chem. Soc.* **2005**, *127*, 16396−16397.
(24) Yamaguchi, T.; Tobe, N.; Matsumoto, D.; Arakawa, H. *Chem. Commun.* **2007**, No. Issue 45, 4767−4769.
(25) Yamaguchi, T.; Tobe, N.; Matsumoto, D.; Nagai, T.; Arakawa, H. *Sol. Energy Mater. Sol. Cells* **2010**, *94*, 812−816.
(26) Miao, Q.; Wu, L.; Cui, J.; Huang, M.; Ma, T. *Adv. Mater.* **2011**, *23*, 2764−2768.
(27) Boschloo, G.; Lindström, H.; Magnusson, E.; Holmberg, A.; Hagfeldt, A. *J. Photochem. Photobiol., A* **2002**, *148*, 11−15.
(28) Halme, J.; Saarinen, J.; Lund, P. *Sol. Energy Mater. Sol. Cells* **2006**, *90*, 887−899.
(29) Zhang, D.; Li, X.; Li, H.; Chen, S.; Sun, Z.; Yin, X.; Huang, S. *Carbon* **2011**, *49*, 5382−5388.
(30) Shin, H.; Lee, H.; Sung, J.; Lee, M. *Appl. Phys. Lett.* **2008**, *92*, 233107.
(31) Lee, H.; Shin, H.; Jeong, Y.; Moon, J.; Lee, M. *Appl. Phys. Lett.* **2009**, *95*, 071104.
(32) Yoo, H.; Shin, H.; Sim, B.; Kim, S.; Lee, M. *Nanotechnology* **2009**, *20*, 245301.
(33) Miskys, C. R.; Kelly, M. K.; Ambacher, O.; Stutzmann, M. *Phys. Status Solidi C* **2003**, 1627−1650.
(34) Yu, I. G.; Kim, Y. J.; Kim, H. J.; Lee, C.; Lee, W. I. *J. Mater. Chem.* **2010**, *21*, 532−538.
(35) Fillinger, A.; Soltz, D.; Parkinson, B. *J. Electrochem. Soc.* **2002**, *149*, A1146−A1156.
(36) Wang, Q.; Moser, J.-E.; Grätzel, M. *J. Phys. Chem. B* **2005**, *109*, 14945−14953.